

A HYDRODYNAMIC METHODOLOGY AND CFD ANALYSIS FOR PERFORMANCE PREDICTION OF STEPPED PLANING HULLS

Hassan Ghassemi, Assoc. Prof.
Mojtaba Kamarlouei, M. Sc.
Sajad Taj Golah Veysi, M. Sc.
Amirkabir University of Technology, Tehran, Iran

ABSTRACT

Nowadays all efforts in planing hull research are focused on resistance reduction for achieving the highest speed in fast planing crafts. Furthermore, many fruitful research projects have been carried out on marine coatings, planing equipment, and optimization of propeller and hull form, which revolutionized industry of high - speed crafts and made them an efficient survival vehicle in coastal areas and rivers. In this paper the hydrodynamic performance of planing hulls are investigated by means of a modified Savitsky model for both non-stepped and stepped bodies. Meanwhile, in order to meet this goal reasonably, effective geometrical parameters of planing hull are investigated and then operational hydrodynamic characteristics of the craft are predicted by using a computational program. Finally, the calculation results are verified by means of a CFD- analysis model.

Keywords: Planing hull, Hydrodynamic performance, CFD analyzed

Introduction

Generally, there are three types of hulls in marine transport industry. Displacing hulls, semi-planing hulls and planing hulls. All of them can be however considered displacing ones when cruising at a low speed. Planing hulls, unlike the other two kinds, are obviously lifted by hydrodynamic pressure, instead of hydrostatic pressure. This goal is achieved by hull design considerations which help the vehicle to rise partially out of the water, then the wetted area reduces considerably that results in frictional drag reduction and subsequent rise of speed of the vehicle.

Nowadays planing vessels are applied as patrol boats, sport fishing vessels, service crafts, ambulances and rescue crafts, recreational and sport crafts. The geometry of stepped planing hull can be considered as two distinct planing bodies merged together close to the waterline. The theory of stepped planing hulls is the same as for simple planing vessels. However this theory cannot be used for afterbody of stepped ones because this part is faced with a disturbed free surface generated by forebody wake. The most significant characteristic feature of stepped planing hulls is the separation of the flow off the step at high speed, leading to partial ventilation of the afterbody, reducing the wetted surface and, consequently, hull resistance

without significant affecting the hydrodynamic lift. Therefore, the ventilated length is shortest along the keel. It increases with speed and is connected with the height of the keel in the flow attachment area above the keel, before the step[1].

It is generally known that step would be an advantageous item in planing hull design. For example, when the owner needs a specific weight distribution, or when a special type of propulsion system and power generation package are going to be applied in planing vessel, the best concept which meets these parameters is a stepped planing hull. On the other hand, the peak of total resistance in such vessels are lower than non-stepped ones. Fig. 1 (A) illustrates a stepped planing hull which is equipped with a free-surface-piercing propeller and ventilating rudder.

Despite, there is no adequate method for performance prediction of stepped planing hulls yet; nowadays most of the planing hulls are designed with step. Meanwhile, two methods may be used for hydrodynamic analysis of stepped planing hulls. The first method is to use computation fluid dynamics (CFD) and the second is to apply an experimental method which needs a model basin and other test facilities.

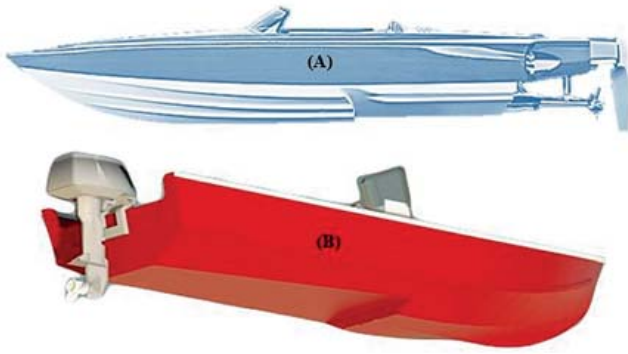


Fig. 1. Stepped planing hull

Literature review

In one of the most famous research investigations on planing hulls, carried out by professor Savitsky in 1964, were introduced some mathematical approaches for frictional and pressure resistance, trim angle and some other hydrodynamic parameters based on a group of experiments done for the first time [2]. Before Savitsky's research, in 1963, Clement and Blount planned some experiments for investigation of the resistance and trim in five 62-series bodies [3]. In 2003 Savander and Rhee applied a numerical method for hydrodynamic parameters of planing hulls and verified their calculation outputs with experimental results [4]. Ghassemi and Ghiasi, in 2007, introduced a complex numerical method which includes both finite element and boundary element approaches to predict the hydrodynamic characteristics of planing hulls [5]. Simultaneously, Brizzolara and Serra studied numerically a fixed-position planing hull and compared the results with available experimental data. An average error of 10% in total drag prediction and 5% error in total lift prediction, showed the capability of numerical methods to obtain accurate results for planing hulls [6]. After that, in 2010, Ghassemi and Kohansal applied a numerical method based on boundary element method to investigate hydrodynamic parameters of different hull shapes [7]. Savitsky and Morabito, in 2010, investigated the wake produced by a step in afterbody of a stepped planing hull [8]. Svahn, in 2009, investigated lift distribution in mono-hulls, basing on Savitsky model, but introducing a great novelty consisted in consideration of a deadrise angle and local trim for afterbody of his model [9]. Garland and Maki, in 2012, did a numerical study on Two-Dimensional Stepped Planing Surface. Their results show that the lift-to-frictional-drag ratio varies very little with respect to the step location [10]. The determining of the hydrodynamic forces on the multi-hull tunnel vessel in steady motion has been investigated by Ghassabzadeh and Ghassemi. Their results included pressure distribution, trim angle, rise of centre of gravity and resistance at various speeds [11]. Recently, Radojcic et al. [12] presented a mathematical model of calm-water resistance for contemporary planing hull forms based on the USCG and TUNS series. They derived two speed-dependent mathematical models, simple and complex, to evaluate the calm-water resistance.

In this paper the main goal is to investigate the hydrodynamic characteristics of planing hulls including stepped and non-stepped models against the change of geometrical parameters of the planing body, with the use of a modified Savitsky model. In this paper, L_p , i.e. the distance measured from transom along keel to the place where normal force acts, and LCG, i.e. position of the centre of gravity, are not considered to be located in the same point as in case of analysis of a hull without step. Additionally, Φ , i.e. the part of weight carried by the forebody of stepped planing hull is not considered a constant value and differs. Finally the applied model results have been verified with CFD calculations for a specific model at different Froude numbers.

Non-stepped planing hull

In this paper, to meet an acceptable result for non-stepped planing hulls a computational program based on a modified Savitsky method, has been developed. Indeed, Savitsky method is based on a kinematic model test of planing hulls and is strongly supported by experimental data [2]. Also the most significant index of this computational algorithm would be the lift coefficient acting on deadrise of the vehicle, $C_{L\beta}$, which is not a constant value and changes in each iteration in order to find the best value. Fig. 2 shows the forces acting on the planing hull and its parameters, where a , c and f are the arms of moments of drag, thrust and lift force, respectively; τ and ε are the angle of trim and thrust line inclination relative to keel line, respectively.

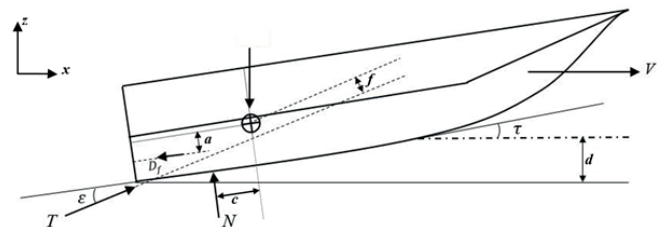


Fig. 2. Diagram of forces acting on non-stepped planing hull in vertical plane

Calculation method and flow-chart

Stability equations for non-stepped planing hulls in longitudinal and vertical directions and in the centre of gravity can be defined as follows, according to Fig. 2:

$$\text{Longitudinal forces: } T \cos(\tau + \varepsilon) - N \sin \tau - D_f \cos \tau = 0 \quad (1)$$

$$\text{Vertical forces: } N \cos \tau + T \sin(\tau + \varepsilon) - mg - D_f \sin \tau = 0 \quad (2)$$

$$\text{Vertical moments with respect to centre of gravity: } N \cdot c + D_f \cdot a - T \cdot f = 0 \quad (3)$$

Undoubtedly, in each numerical computation method convergence condition plays a markedly role for achieving both reasonable outputs and CPU time. In this paper two constraint conditions are considered.

The first condition, Eq. (4), defines a satisfactory convergence of vertical moment computation.

$$F_{L\beta} L_p - mg LCG \leq \zeta_1 \quad (4)$$

where:

$$F_{L\beta} = \frac{1}{2} \rho U^2 B^2 C_{L\beta} \quad (5)$$

and L_p is calculated as follows:

$$L_p = 0.75 - \frac{\lambda B}{5.21 C_v^2 + 2.39 \lambda^2} \quad (6)$$

While ρ is water density, U – vehicle speed, B - vehicle breadth and λ - mean wetted length-to-beam ratio.

The second condition is a satisfactory convergence of trim calculation, expressed by Eq. (7).

$$M_{tot} = mg \left[\frac{c}{\cos \tau} (1 - \sin \tau (\sin(\tau + \varepsilon)) - f \sin \tau) \right] + D_f (a - f) \leq \zeta_2 \quad (7)$$

where ζ_1 and ζ_2 are constants assumed to be as little as $1e-2$.

The flow chart of the modified Savitsky method is shown in Fig. 3. As it can be seen, two constraints should be satisfied in order to finish the calculation cycle.

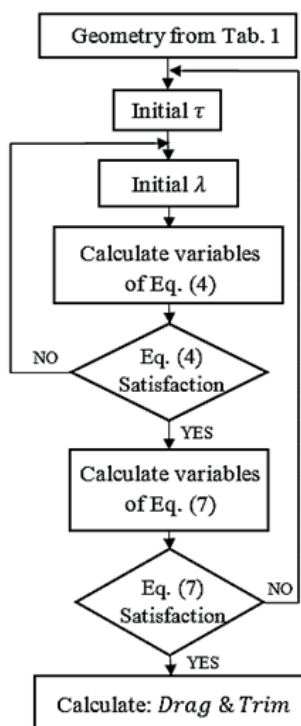


Fig.3. Flow chart of the calculation acc. the assumed method

Calculation results

The output for an examined model is presented to show the effects of deadrise angle, longitudinal position of centre of gravity (LCG), and $\frac{L}{B}$ ratio on trim and $\frac{Drag}{L\beta}$ ratio in a given range of Froude number values. The model parameters are specified in Tab. 1.

Tab.1. Geometrical parameters of examined vehicle

| Parameter | Value |
|---|------------|
| Displacement (Δ) | 18.7 (t) |
| Deadrise angle (β) | 13 (deg) |
| Breadth (B) | 3.807 (m) |
| Longitudinal Centre of Gravity (LCG from aft) | 6.695 (m) |
| Vertical Centre of Gravity (VCG) | 0.8 (m) |
| Length -to - Breadth ratio ($\frac{L}{B}$) | 4.09 |
| Distance between T and centre of gravity (measured normal to T) | 0.0380 (m) |
| Thrust- line inclination angle relative to keel -line | 10 (deg) |

Tab. 2 shows results of the verification. The trim calculated by using the prepared program and the reference trim achieved from a given program [13] are compared to each other and the respective error values at different speeds are presented in 4th row of Tab. 2.

Tab. 2. Comparison between program output and reference results[13].

| Speed (Knots) | 15 | 20 | 25 | 30 | 35 | 40 | 45 |
|--------------------------|------|------|------|------|------|------|------|
| Calculated trim (degree) | 2.4 | 2.96 | 3.3 | 3.26 | 3 | 2.67 | 2.36 |
| Reference trim (degree) | 2.53 | 3.03 | 3.36 | 3.33 | 3.07 | 2.74 | 2.41 |
| Error (%) | 5.13 | 2.31 | 1.78 | 2.1 | 2.28 | 2.55 | 2 |

Moreover, Fig. 4 shows the change of hydrodynamic parameters against the change of geometrical characteristics in a given range of Froude number values. Also, the effect of deadrise angle, longitudinal centre of gravity and $\frac{L}{B}$ ratio on trim angle and $\frac{Drag}{L\beta}$ ratio at different Froude number values is indicated in this figure, respectively. Obviously, in case of non-stepped planing hulls the increase of deadrise angle and LCG result in trim angle reduction and drag enhancement. On the contrary, the increase of $\frac{L}{B}$ ratio rises the trim angle and decreases the $\frac{Drag}{L\beta}$ ratio.

Stepped planing hull

As it can be seen in Fig. 7, the body of stepped planing hulls is divided into two parts, fore and aft, and hydrodynamic forces and moments affect each part distinctly. The first reason for using stepped planing hull is to divide the wetted surface into smaller parts. For instance, in case of a single-step

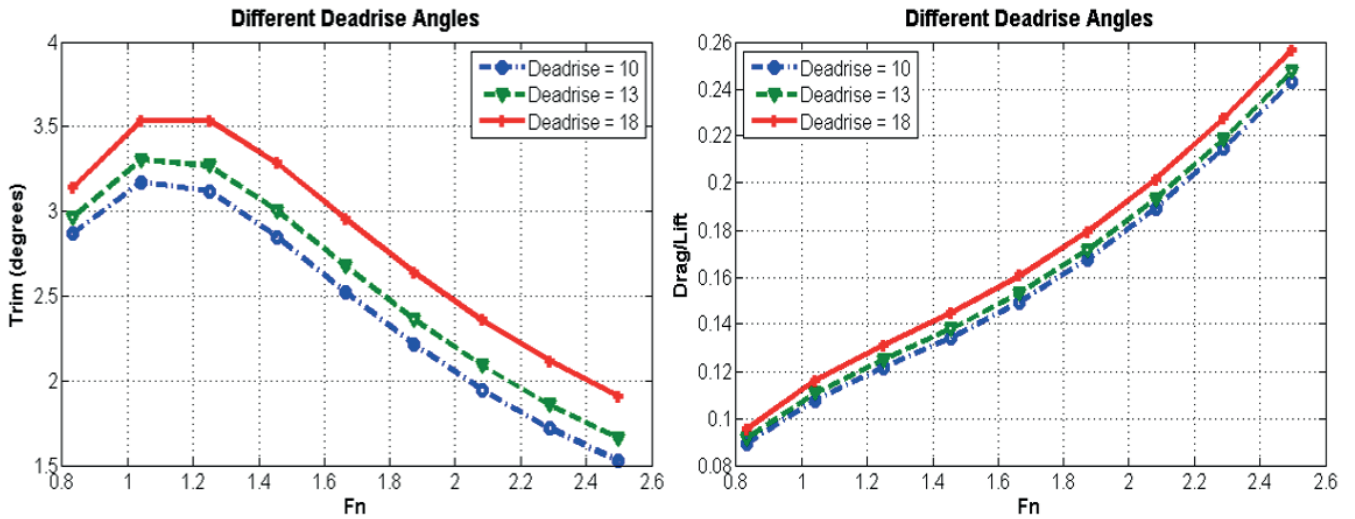


Fig.4. The change of trim and $\frac{Drag}{Lift}$ ratio in function of Froude number F_n for three deadrise angle values

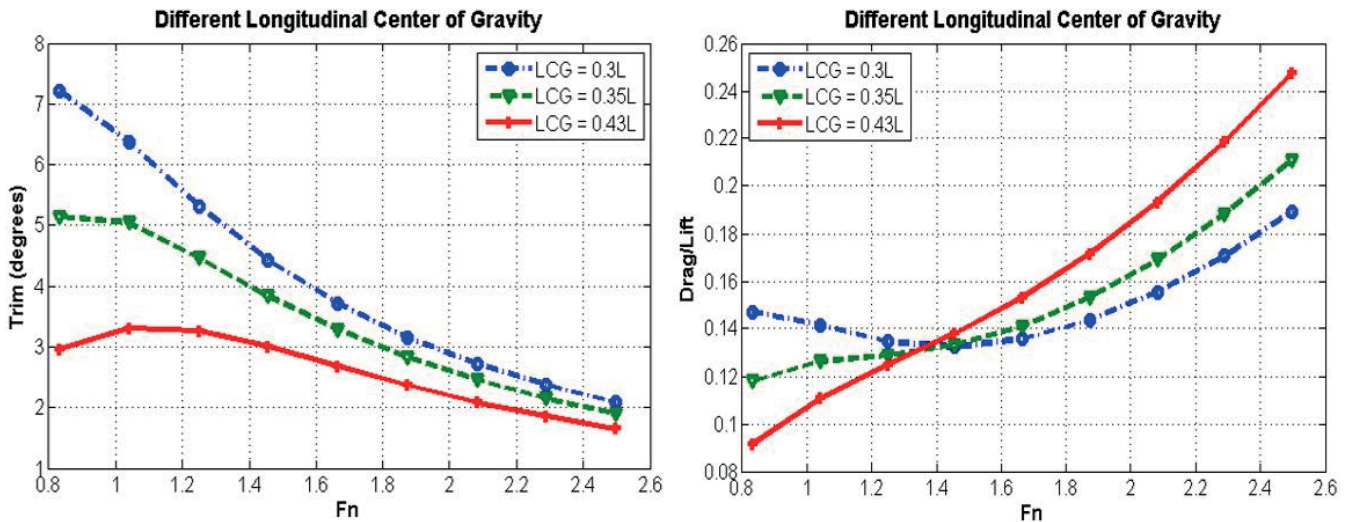


Fig.5. The trends of trim and $\frac{Drag}{Lift}$ ratio in function of Froude number F_n for three LCG values

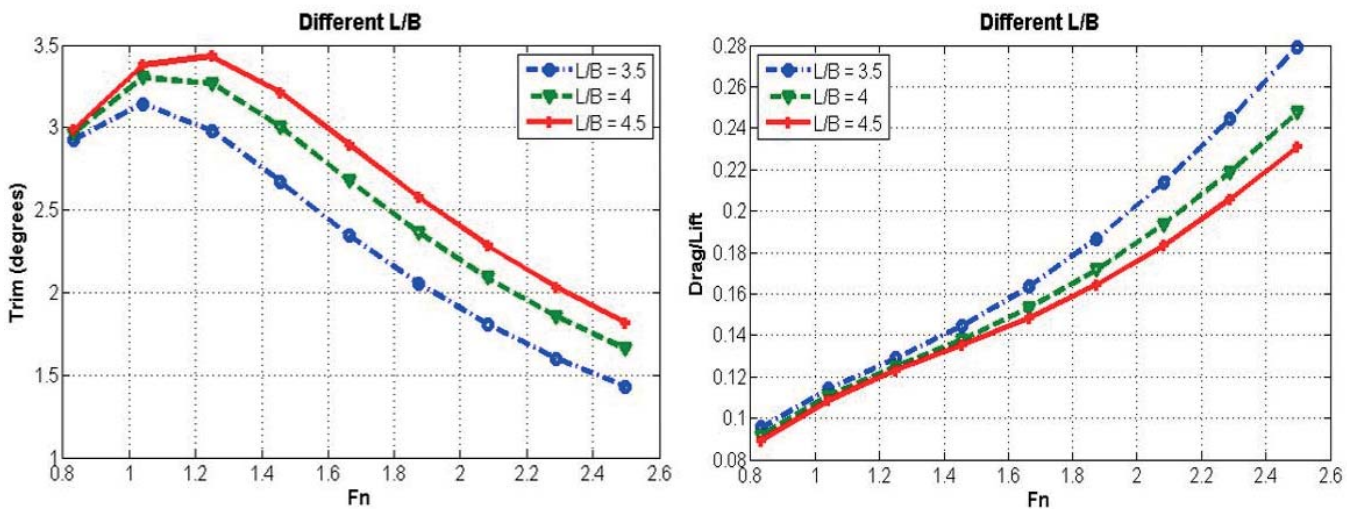


Fig. 6. The variation of trim and $\frac{Drag}{Lift}$ ratio in function of Froude number F_n for three $\frac{L}{B}$ values

planing hull its wetted surface is divided into two smaller areas. Therefore, as a result, amount of the lift generated in stepped planing hulls is markedly greater than lift force generated in case of a long continuous wetted surface in non-stepped ones. So this growth in lift force causes an efficient reduction of wet surface resulting in reduction of the frictional resistance. And, Φ is the weight proportion assigned to forebody, and two indexes, 1 and 2, stand for forebody and afterbody properties, respectively.

Hydrodynamics of afterbody

To estimate the wetted area of aft hull, it is obvious that wake field of forebody and its boundaries should be investigated. Wetted area of afterbody which is affected by forebody wake field can be seen in Fig. 7.

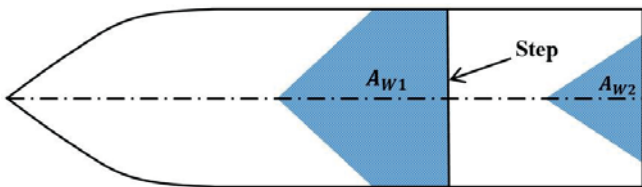


Fig. 7. Wetted area of forebody and afterbody of stepped planing hull

Savitsky and Morabito investigated the afterbody wake generated by step in a stepped planing hull and achieved some semi-experimental relations for the wake behind the step, using model tests. Basically, two important parameters resulting from their experiment, are X_{CL} and $X_{\frac{1}{4}}$. The first represents the distance between step and afterbody wetted surface, measured along keel line, and the other is that measured in one fourth of beam from the keel line. Local level waterline is also an effective parameter which is formed by a straight line connecting the first point of wetted surface in keel line and the first one in the $\frac{1}{4}$ of beam. Fig. 8 shows the three quantities.

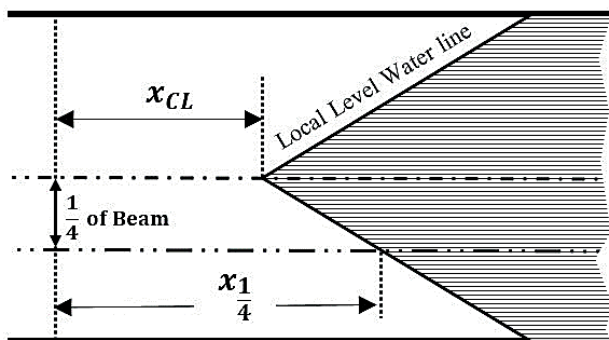


Fig. 8. Local waterline as a result of wake generated by step

Moreover, besides this difference in shape, it is assumed that the water behaves the same way meeting the aft hull as it does when hitting the fore hull. Then, to meet reasonable

results the effects of wake on afterbody are considered by using definition of some local parameters with L index such as β_{2L} which is local deadrise angle in aft hull. Actually, this angle is the difference between β and the inclined waterline in the afterbody due to wake field.

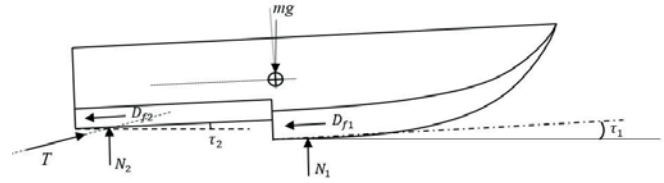


Fig. 9. Diagram of forces acting on stepped planing hull

Generally, pressure and frictional resistances are two greater parts of total resistance which includes spray, wave generation and other particular terms of resistance. Eq. (8) and (9) are used to estimate pressure and frictional resistance in forebody of stepped planing hull, respectively.

$$R_{p1} = \Phi mg \tan \tau_1 \quad (8)$$

$$D_{f1} = 0.5 \frac{\rho V_{m1}^2 \lambda_1 b_1^2}{\cos \beta} (C_f + \Delta C_f) \quad (9)$$

$$D_1 = \Phi mg \tan \tau_1 + \frac{D_{f1}}{\cos \tau_1} \quad (10)$$

The same for afterbody:

$$R_{p2} = (1 - \Phi) mg \tan \tau_2 \quad (11)$$

$$D_{f2} = 0.5 \frac{\rho V_{m2}^2 \lambda_2 b_2^2}{\cos \beta} (C_{f2} + \Delta C_f) \quad (12)$$

$$D_2 = (1 - \Phi) mg \tan \tau_2 + \frac{D_{f2}}{\cos \tau_2} \quad (13)$$

And, N_1 and N_2 are lift forces on forebody and afterbody which can be calculated by using well-known equations.

Methodology and calculation flow chart

Stability equations for stepped planing hulls in longitudinal and vertical directions and in the centre of gravity can be defined according to Fig. 9 as follows:

$$\text{Longitudinal forces: } T \cos(\tau_2 + e) - N_1 \sin \tau_1 - N_2 \sin \tau_2 - D_{f1} \cos \tau_1 - D_{f2} \cos \tau_2 = 0 \quad (14)$$

$$\text{Vertical forces: } N_1 \cos \tau_1 + N_2 \cos \tau_2 + T \sin(\tau_2 + e) - mg - D_{f1} \sin \tau_1 - D_{f2} \sin \tau_2 = 0 \quad (15)$$

$$\text{Vertical moments with respect to centre of gravity: } N_1 c_1 + N_2 c_2 + D_{f1} a_1 + D_{f2} a_2 - Tf = 0 \quad (16)$$

And, the convergence conditions in this program are the same as in the case of non-stepped hulls. The main equations of force and moment differ in this section.

The first constraint equation for vertical forces is as follows:

$$F_{L1} + F_{L2} - mg \leq \zeta_2 \quad (17)$$

And the second constraint is the condition for a satisfactory convergence of moment calculations, which means that should be a definite positive value.

$$M_{total} = N_1c_1 + N_2c_2 + D_{f1}a_1 + D_{f2}a_2 - T \quad f \geq 0 \quad (18)$$

where a, c and f are the coefficients formerly defined. The calculation flow chart is shown in the Fig. 10. As shown in the chart, two constraints should be satisfied before the calculation processes are finished.

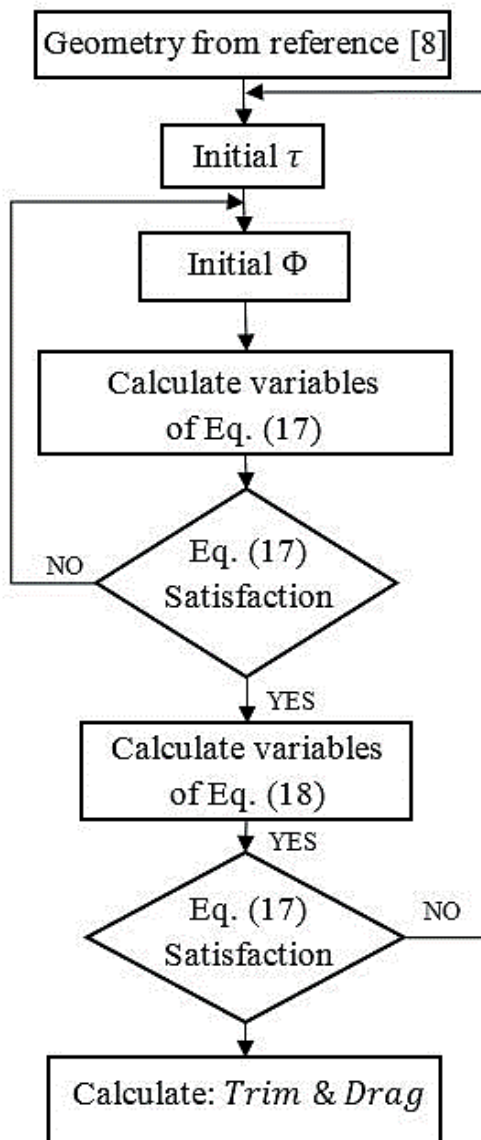


Fig. 10. Flow chart of the calculation program for stepped planing hulls

Calculation results

Results obtained from the algorithm based on the modified Savitsky method for stepped planing hulls, concern a single-step planing hull. Then, the results are verified by using output from the precise model [9].

First, some basic characteristics of the selected planing hull are determined as follows:

| | | |
|-------------------------------|---------------|------------------------|
| HS = 0.05 (m) | e = 0.15 (m) | b ₁ = 2 (m) |
| m = 4000 (kg) | LS = 2.5 (m) | b ₂ = 2 (m) |
| β ₁ = 11 (degrees) | LCG = 2.6 (m) | V = 35 (knot) |
| β ₂ = 10 (degrees) | VCG = 0.5(m) | |

Then a comparison between calculation results based on the prepared program and reference output, is done. Tab.3 shows trim angle, total resistance, and required power values obtained from both the program and reference model.

Tab. 3. Comparison between calculation program results and reference output [9].

| Parameter | Reference calculations | Acc. prepared program | Error (%) |
|----------------------|------------------------|-----------------------|-----------|
| Trim (degrees) | 4.4 | 4.36 | 1 |
| Total Resistance (N) | 5229 | 5154.1 | 1.4 |
| Required power (HP) | 128 | 124.5 | 2.7 |

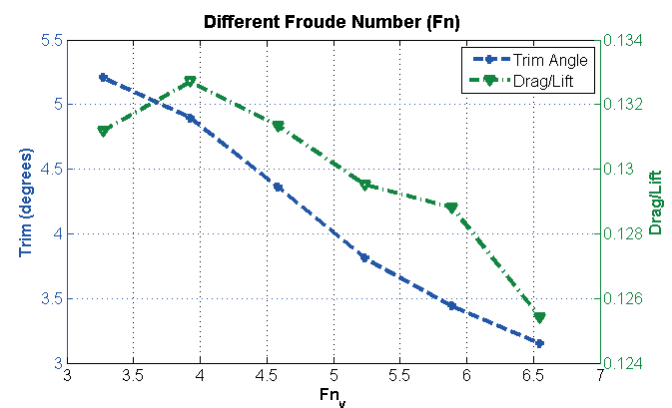


Fig. 11. The effect of volumetric Froude number on trim and $\frac{Drag}{Lift}$ ratio

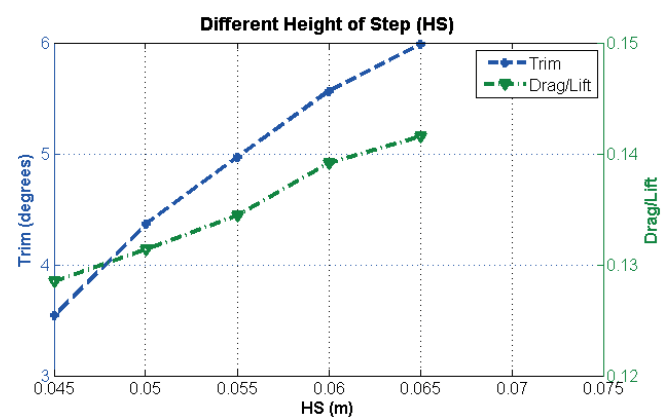


Fig. 12. The effect of the step height HS on trim and $\frac{Drag}{Lift}$ ratio

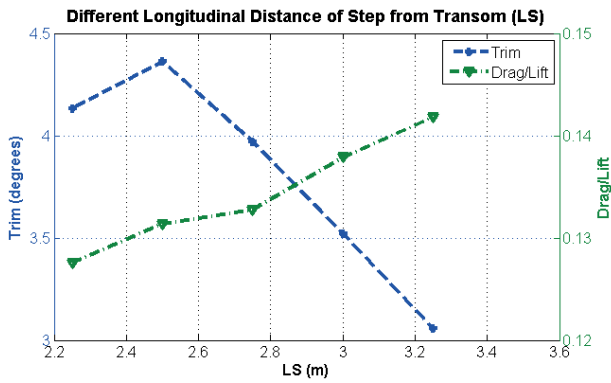


Fig. 13. The effect of the longitudinal distance of step LS on trim and $\frac{Drag}{Lift}$ ratio

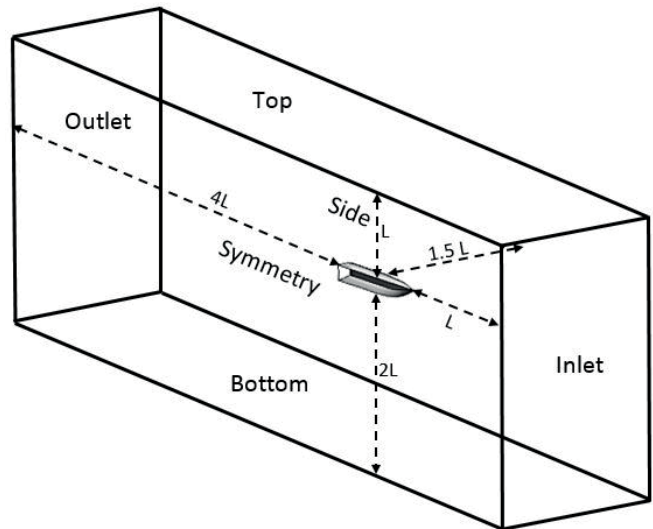


Fig. 15. Boundary condition definition

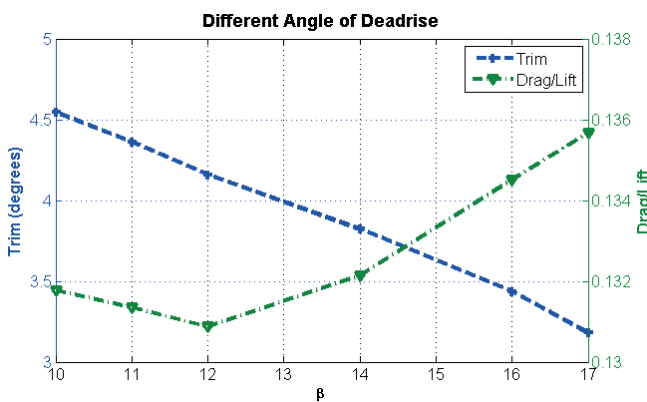


Fig. 14. The effect of deadrise angle on trim and $\frac{Drag}{Lift}$ ratio

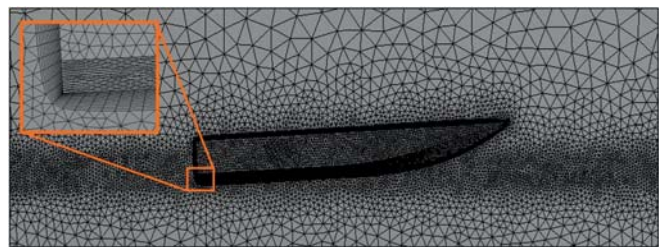


Fig. 16. FE mesh generated around the hull and within boundary layer

Generally, as can be seen in Fig. 11, in stepped planing hulls the amount of trim and $\frac{Drag}{Lift}$ ratio decreases with the increase of volumetric Froude number value. Also the effect of the step height (HS), longitudinal distance of step from transom (LS), and deadrise angle on these two markedly important parameters, is shown in Fig. 12, 13, and 14, respectively.

CFD analysis

The steady-state simulation has been carried out with the use of ANSYS CFX v.14 software. The boundary condition is divided into the parts, as shown in Fig. 15. As it can be seen in the figure the dimensions are so assumed as to achieve more adequate results.

To model the turbulent flow, the standard $K - \epsilon$ is applied and a homogeneous water/air multiphase finite volume approach is used for modelling the free surface. Also a half body is only analysed in order to reduce the CPU time. Furthermore, an unstructured mesh with 5.1M elements is generated, and to obtain a reasonable Y^+ , under 50, a specific boundary layer mesh is applied to near-wall regions. Obviously, for precise free surface modelling, number of mesh elements in free surface and water separation regions is assumed greater.

Before discussing CFD results and verification process, the following contours indicating the computed wave pattern at different Froude number values, are shown. As it can be seen in Fig. 17 the increasing Froude number values results in wave length growth, that leads to wave angle reduction.

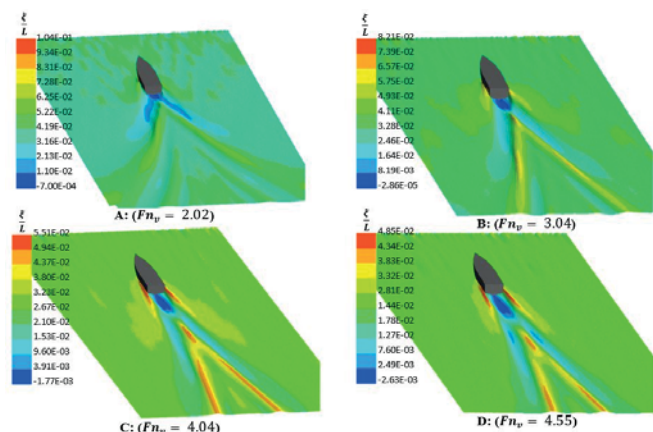


Fig. 17. Wave patterns at different volumetric Froude number values

Additionally, Fig. 18 shows pressure distribution on the stepped hull bottom surface. As shown in the Fig. 18 and 19, the points (A), (B), and (C) represent the peak pressure position in the afterbody, step and forebody, respectively.

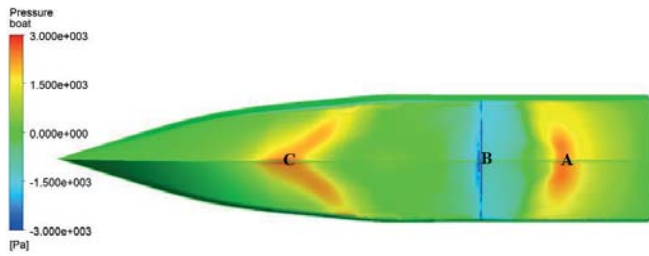


Fig.18. Pressure distribution contours on the bottom surface of stepped planing hull at $Fn_v = 5.89$

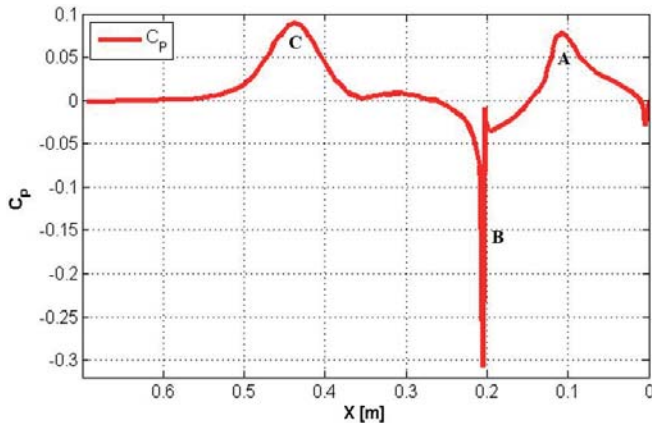


Fig. 19. Pressure coefficient distribution along the keel line of stepped planing hull at $Fn_v = 5.89$

Comparison between CFD and program results

To verify the program results thoroughly, CFD results are compared with program output. As can be seen in the following figures, CFD results are presented for various volumetric Froude number values for both non-stepped and stepped hull. And, in Tab. 4 the error values are shown. The minimum error values occur at $Fn_v = 2.02$ and $Fn_v = 5.89$, and the maximum ones - at $Fn_v = 4.55$ and $Fn_v = 5.23$ for non-stepped and stepped hull, respectively.

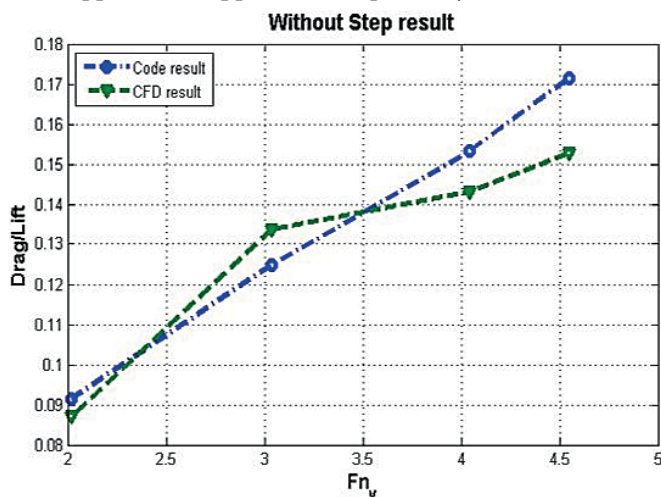


Table 4: Error values in function of volumetric Froude number

| | Volumetric Froude Number | Drag/Lift (code) | Drag/Lift (progr.) | Errors (%) |
|------------------|--------------------------|-------------------|---------------------|------------|
| Non-stepped hull | 2.02 | 0.092 | 0.087 | 4.3 |
| | 3.04 | 0.125 | 0.134 | 7.2 |
| | 4.04 | 0.153 | 0.143 | 6.6 |
| | 4.55 | 0.171 | 0.152 | 10.1 |
| Stepped hull | 3.27 | 0.131 | 0.121 | 7.8 |
| | 3.92 | 0.133 | 0.141 | 6.3 |
| | 5.23 | 0.129 | 0.144 | 12.2 |
| | 5.89 | 0.128 | 0.122 | 4.2 |

Conclusions

To conclude, in this work all efforts have been focused on achieving the best algorithm based on practical equations for both non- stepped and stepped planing hulls. Furthermore the effect of geometrical parameters on the performance of planing hulls, has been investigated. The obtained results show that in non- stepped planing hulls the increase of deadrise angle and LCG result in a drag rise and trim decline. On the contrary, ratio increase rises trim angle and decreases drag. On the other hand, for stepped planing hulls the rising of step height causes a significant rise in both drag and trim. Also the increase of deadrise angle and step-to-transom distance leads to drag increase and trim decrease. Finally the results obtained from the prepared program are reasonably proved by the performed CFD analysis.

Acknowledgement

This research was supported by the Marine Research Center of Amirkabir University of Technology whose efforts are greatly acknowledged.

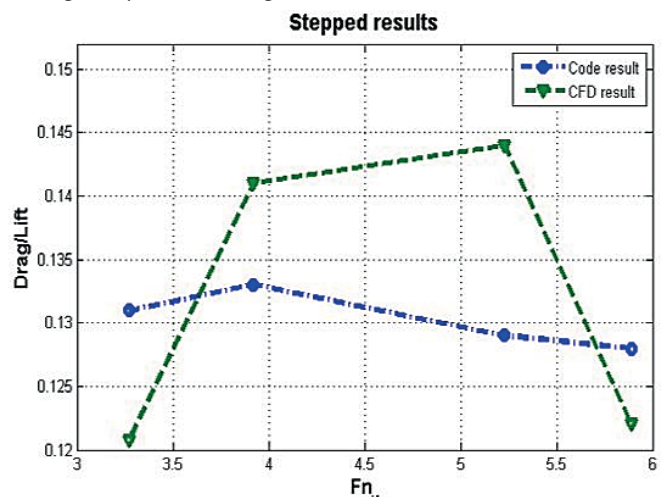


Fig. 20. Comparison between program (code) and CFD results in function of volumetric Froude number.

Bibliography

CONTACT WITH AUTHORS

1. O. M. Faltinsen: Hydrodynamics of High-Speed Marine Vehicles, Cambridge University Press, 2005.
2. D. Savitsky: Hydrodynamic Design of Planning Hull, Marine Technology, vol. 1, no. 1, pp. 71-95, 1964
3. C. E. P and B. D. L: Resistance Tests of a Systematic Series of Planning Hull Forms, Society of Naval Architects and Marine Engineers (SNAME), Hampton, 1963
4. B. R. Savander and S. H. Rhee: Steady Planning Hydrodynamics: Comparison of Numerical and Experimental Results, Fluent Users' Group, Manchester, NH, 2003
5. H. Ghassemi and M. Ghiasi: A Combined Method for the Hydrodynamic Characteristics of Planning Crafts, Ocean Engineering, vol. 35, no. 3-4, pp. 310-322, 2007
6. S. Brizzolara and F. Serra: Accuracy of CFD Codes in the Prediction of Planing Surfaces Hydrodynamic Characteristics, in : 2nd International Conference on Marine Research and Transportation, Naples, 2007
7. A. R. Kohansal and H. Ghassemi: A Numerical Modelling of Hydrodynamic Characteristics of Various Planning Hull Forms, Ocean Engineering, vol. 37, no. 5-6, pp. 498-510, 2010
8. D. Savitsky and M. Morabito: Surface Wave Contours Associated with the Forebody Wake of Stepped Planning Hulls, Marine Technology, vol. 47, no. 1, pp. 1-16, 2010
9. D. Svahn: Performance Prediction of Hulls with Transverse, Marina System Center for Naval Architecture, Stockholm, 2009
10. W. R. Garland and K. J. Maki: A Numerical Study of a Two-Dimensional Stepped Planing Surface, Journal of Ship Production and Design, vol. 28, no. 2, pp. 60-72, 2012
11. M. Ghassabzadeh and H. Ghassemi: Determining of the Hydrodynamic Forces on the Multi-hull Tunnel Vessel in Steady Motion, The Brazilian Society of Mechanical Sciences and Engineering, in press, 2013
12. D. Radojic, A. Zgradic, M. Kalajdzic and A. Simic: Resistance Prediction for Hard Chine Hulls in the Pre-Planing Regime, Polish Maritime Research, vol. 21, no. 2(82), pp. 9-26, 2014
13. H. Holm: Hydrodynamic Design of Planing Hulls- Online Program, Marine Hydrodynamics' Site NTNU University, Trondheim, 2002

Hassan Ghassemi
Sajad Taj Golah Veysi
Mojtaba Kamarlouei

Amirkabir University of Technology
Department of Ocean Engineering
Hafez Ave.
Tehran
IRAN